

# Directed Evolution of the Epidermal Growth Factor Receptor Extracellular Domain for Expression in Yeast

Yong-Sung Kim,<sup>1,3</sup> Rashna Bhandari,<sup>2,4</sup> Jennifer R. Cochran,<sup>1,5</sup> John Kuriyan,<sup>2</sup> and K. Dane Wittrup<sup>1,\*</sup>

<sup>1</sup>*Division of Biological Engineering and Department of Chemical Engineering, Massachusetts Institute of Technology, Cambridge, Massachusetts*

<sup>2</sup>*Howard Hughes Medical Institute, Department of Molecular and Cell Biology and Department of Chemistry, University of California, Berkeley, California*

**ABSTRACT** The extracellular domain of epidermal growth factor receptor (EGFR-ECD) has been engineered through directed evolution and yeast surface display using conformationally-specific monoclonal antibodies (mAbs) as screening probes for proper folding and functional expression in *Saccharomyces cerevisiae*. An EGFR mutant with four amino acid changes exhibited binding to the conformationally-specific mAbs and human epidermal growth factor, and showed increased soluble secretion efficiency compared with wild-type EGFR. Full-length EGFR containing the mutant EGFR-ECD was functional, as assayed by EGF-dependent autophosphorylation and intracellular MAPK signaling in mammalian cells, and was expressed and localized at the plasma membrane in yeast. This approach should enable engineering of other complex mammalian receptor glycoproteins in yeast for genetic, structural, and biophysical studies. *Proteins* 2006;62:1026–1035. © 2005 Wiley-Liss, Inc.

**Key words:** directed evolution; yeast surface display; receptor engineering; epidermal growth factor receptor; fluorescence activated cell sorting; high throughput screening

## INTRODUCTION

The epidermal growth factor receptor (EGFR) is a transmembrane receptor tyrosine kinase which exerts its biological effects in response to binding of specific polypeptide ligands, including epidermal growth factor (EGF) and transforming growth factor- $\alpha$  (TGF- $\alpha$ ).<sup>1,2</sup> The EGFR consists of a 621-residue extracellular ligand binding domain (EGFR-ECD), a 23-residue transmembrane domain, a 250-residue kinase domain, and a 229-residue C-terminal regulatory domain containing several tyrosine residues.<sup>1,3</sup> The ligand binding region of the EGFR-ECD can be divided into four subdomains: I (residues 1–165), II (residues 166–310), III (residues 311–480), and IV (residues 481–621).<sup>4–7</sup> Domains I and III are  $\beta$ -solenoid or  $\beta$ -helix folds, and domains II and IV consist of a number of small modules, connected by one or two disulfide bonds.<sup>4–7</sup> Binding of EGF to the EGFR-ECD leads to homo- or heterodimerization of the EGFR with other receptor family members, activation of the catalytic tyrosine kinase domain, autophosphorylation of specific residues in the

C-terminus, and subsequent cellular signaling.<sup>1,2</sup> Recent crystallographic studies show that ligand binding to the EGFR-ECD induces receptor conformational changes from a tethered, monomeric form to an extended, dimeric complex.<sup>4–7</sup>

Overexpression and oncogenic truncations of the EGFR have been observed in many epithelial carcinomas, including glioblastomas and non-small lung cancer, pancreatic, breast, head and neck, colon, and ovarian cancers.<sup>8,9</sup> Therefore, the EGFR-ECD has been an important target for the development of anti-cancer therapeutics, including monoclonal antibodies (mAbs), small molecules, and peptides.<sup>9,10</sup> Recent crystallographic studies of the EGFR-ECD have provided significant insight into receptor–ligand and receptor–receptor interactions involved in activation of the EGFR.<sup>7</sup> Previously, soluble EGFR-ECD has been successfully produced in mammalian and insect cell expression systems for biophysical and structural studies.<sup>5,6,11,12</sup> The establishment of a robust and rapid microbial-based expression system would allow for production of large quantities of functional EGFR-ECD and facilitate genetic manipulation for mutational studies. The EGFR-ECD contains 25 disulfide bonds and 12 potential N-linked glycosylation sites,<sup>3,4,6</sup> which makes it poorly suited for expression in bacterial systems. Yeast cells have a more sophisticated quality control system in their protein secretion pathway that can perform eukaryotic-specific proteolytic processing, chaperone-assisted folding,

**Abbreviations:** EGFR-ECD, the extracellular domain of human epidermal growth factor receptor; hEGF, human epidermal growth factor; mAb, monoclonal antibody; FACS, fluorescence activated cell sorting.

\*Correspondence to: K. Dane Wittrup, Division of Biological Engineering and Department of Chemical Engineering, Massachusetts Institute of Technology, 400 Main St. Bldg 66-552, Cambridge, MA 02139. E-mail: wittrup@mit.edu

Yong-Sung Kim's present address is the Department of Molecular Science and Technology, Ajou University, Korea.

Rashna Bhandari's present address is the Department of Neuroscience, Johns Hopkins School of Medicine, Baltimore, MD 21205.

Jennifer R. Cochran's present address is the Department of Bioengineering, Stanford University, Stanford, CA 94305.

Received 5 January 2005; Revised 29 March 2005; Accepted 30 March 2005

Published online 14 December 2005 in Wiley InterScience (www.interscience.wiley.com). DOI: 10.1002/prot.20618

and post-translational modifications, such as disulfide-bond formation, and certain types of glycosylation.<sup>13,14</sup>

Directed evolution by random mutagenesis and recombination followed by screening or selection is a powerful tool to optimize protein function, stability, expression, recognition (e.g., affinity), and solubility.<sup>15,16</sup> Yeast surface display technology has been used to engineer proteins for increased ligand binding affinity,<sup>17</sup> and increased protein stability and expression levels of ectodomains of the T cell receptor,<sup>18,19</sup> TNF receptor,<sup>20</sup> and MHC.<sup>21</sup> Rational site-directed mutagenesis was used to increase the soluble expression of a homogeneous form of the extracellular domain of erythropoietin receptor in *Pichia pastoris*.<sup>22</sup>

We determined that the wild type EGFR-ECD is expressed on the yeast cell surface in a partially misfolded form. Here we use directed evolution and yeast surface display to isolate mutants that exhibit proper protein folding for the soluble expression of EGFR-ECD in *Saccharomyces cerevisiae*. As screening probes, several conformationally-specific mAbs against EGFR-ECD were employed.<sup>23</sup> One EGFR-ECD mutant (404SG) with the amino acid changes A62T, L69H, F380S, and S418G, showed similar yeast surface expression levels compared with wild-type EGFR-ECD, but exhibited binding to all conformationally-specific mAbs tested, and the ligand hEGF. Soluble expression of the 404SG EGFR-ECD mutant in yeast produced homogeneously glycosylated protein with a yield of 4–6 mg/L. Unlike soluble wild-type EGFR-ECD produced in yeast, the soluble 404SG mutant exhibited an hEGF binding affinity comparable to previously published values for soluble hEGF-EGFR complexes. Full-length EGFR proteins containing the mutant EGFR-ECDs were competent to bind ligand and initiate intracellular signaling cascades when transfected into mammalian cells. In addition, these full-length EGFR mutant proteins were shown to be well expressed in yeast and to localize to the plasma membrane. These studies demonstrate that it is possible to engineer the expression of functional, folded glycoproteins in yeast, and pave the way for structural and functional studies of complex mammalian proteins in yeast for facile genetic studies.

## MATERIALS AND METHODS

### Materials and Media

Raw ascites fluid containing the c-myc monoclonal antibody (mAb) 9E10 was purchased from The Hybridoma Bank at the University of Iowa. The anti-human EGFR mAbs 225, 528, and 199.12 were purchased from LabVision (Fremont, CA), EGFR1 from Biotools International (Saco, Maine), and mAb ICR10 from Abcam Limited (Cambridge, UK). The anti-human EGFR mAb 2D2 was a generous gift from Nita J. Maihle at the Mayo Cancer Center, and the mAb 13A9 was provided by Genentech (San Francisco, CA). Alexa-488 labeling kit was from Molecular Probes (Eugene, OR). Synthetic selective medium SD-CAA (-ura, -trp) contained 20 g/L glucose, 6.7 g/L yeast nitrogen base without amino acids (Difco, MD), 5.4 g/L Na<sub>2</sub>HPO<sub>4</sub>, 8.6 g/L NaH<sub>2</sub>PO<sub>4</sub> · H<sub>2</sub>O, and 5 g/L casamino acids (Difco, MD). Synthetic selective SD-SCAA (-ura, -trp,

-leu) was also prepared in same way, except 3.9 g/L SCAA synthetic amino acids were used instead of the casamino acids.<sup>24</sup> SG-CAA and SG-SCAA contained the same composition as SD-CAA and SD-SCAA, respectively, except glucose was replaced with galactose.

### Cloning of EGFR-ECD Genes and Construction of Mutant Libraries

The open reading frame of the extracellular domain (residues 1–621) of human EGFR was subcloned in-frame into the pCTCON<sup>23</sup> and pCAga2 yeast surface display plasmids, generating pNAga2-EGFR-ECD and pCAga2-EGFR-ECD, respectively. The pNAga2-EGFR-ECD and pCAga2-EGFR-ECD have a translational order of N-(Aga2)-(HA tag)-(EGFR-ECD)-(c-myc tag)-C, and N-(EGFR-ECD)-(c-myc tag)-(Aga2)-C, respectively. For the first round of mutagenesis and screening, a library of EGFR-ECD mutants was generated by error prone PCR using the nucleotide analogs 8-oxo-2'-deoxyguanosine-5'-triphosphate and 2'-deoxy-p-nucleoside-5'-triphosphate (TriLink Biotech, CA) as described previously.<sup>25</sup> For the second round of screening, a library of EGFR-ECD mutants was constructed by combining error prone PCR using nucleotide analogs and DNA shuffling.<sup>26,27</sup> DNA templates used for the mutagenesis and shuffling were wild type EGFR-ECD, a double mutant (F380S and S418G) selected from the first round, and the aglycomutant N(12)A, in which the 12 potential EGFR-ECD Asn glycosylation sites were all mutated to Ala.<sup>28</sup> The EGFR-ECD gene libraries (10 µg) were mixed with restriction enzyme digested pNAga2 (1 µg) or pCAga2 (1 µg) backbone vector, and were transformed into the yeast strain EBY100<sup>29</sup> by homologous recombination using a Bio-Rad Gene Pulser electroporation apparatus.<sup>30</sup> Ten parallel transformations generated a library size of approximately 10<sup>8</sup> transformants. Site-directed mutagenesis was performed using a QuickChange mutagenesis kit (Stratagene, CA) following the manufacturer's instructions. All clones were confirmed by DNA sequencing.

### Screening of EGFR-ECD Mutants

Yeast cells were grown in SD-CAA media at 30°C to an OD<sub>600</sub> of 6, pelleted by centrifugation, and transferred into SG-CAA media and grown at 30°C for approximately 20 h to induce the surface expression EGFR-ECD.<sup>18,24,29</sup> Cells from the induced yeast library (10<sup>8</sup>) were incubated with 10 µg/mL of mAb 225, 199.12, or EGFR1 at 37°C with agitation for 30 min in 0.5 mL PBSB [phosphate buffered saline (pH 7.4) containing 1 mg/mL bovine serum albumin (Sigma)]. Since the monoclonal antibodies were all murine, single color indirect immunofluorescence was used in each screening round. Cells were washed with PBSB, and labeled with goat anti-mouse-phycoerythrin (PE) secondary antibody (1:25 dilution, Sigma) for 20 min on ice with frequent mixings. The labeled cells were washed, resuspended with PBSB, and then sorted with gate settings to collect cells with the highest fluorescence levels (~1–2%) on a high speed MoFlo cell sorter (Cytomation Inc., CO). Collected cells were regrown and induced at 30°C as above,

and then subsequently subjected to sorting with alternative single labeling of mAbs 225, 199.12, or EGFR1 until mutants with improved binding to the mAbs were highly enriched (> 6 sequential flow cytometry sorts). Enriched library pools were plated on the selective media and single clones were isolated and characterized with the anti-c-myc ascites 9E10, and the EGFR-specific mAbs 199.12, EGFR1, ICR10, 225, 528, 13A9, and 2D2.

### EGF Binding Assays and Thermal Stability Measurements

Human epidermal growth factor (hEGF) from Pepro-Tech (NJ) was used without further purification and its concentration was determined by the extinction coefficient of  $14,400 \text{ M}^{-1}\text{cm}^{-1}$  at 280 nm.<sup>12</sup> The apparent dissociation constant ( $K_D$ ) of hEGF binding to yeast surface displayed EGFR-ECD was determined by competition binding with mAb 225 as described previously.<sup>23</sup> Varying concentrations of hEGF (0–161  $\mu\text{M}$ ) and 3 nM of mAb 225 were incubated with yeast cells displaying EGFR-ECDs at 25°C for 90 min with gentle agitation. After washing with PBSB, and a secondary labeling with goat anti-mouse-PE, the remaining fraction of bound mAb 225 was determined by indirect immunofluorescence using a Coulter Epics XL flow cytometry. Assuming that hEGF and the mAb 225 compete for a single binding site of EGFR-ECD,<sup>31</sup> data were analyzed to obtain apparent  $K_D$  values of hEGF binding to EGFR-ECDs as previously described.<sup>23</sup> For the determination of thermal stability of yeast surface displayed EGFR-ECDs,  $10^6$  yeast cells/mL were pelleted, resuspended in 100  $\mu\text{L}$  PBSB, and incubated at a range of temperatures (20–80°C) for 20 min, and then immediately cooled at 4°C for 10 min.<sup>32</sup> The relative amount of properly folded EGFR-ECD remaining on the cell surface was determined by mAb 199.12 and 225 labeling using flow cytometry.<sup>23</sup>

### Soluble Production of EGFR-ECDs

DNA encoding the EGFR-ECDs was subcloned into pRS GAL, a yeast secretion plasmid which has a GAL promoter, an N-terminal synthetic PrePro sequence for targeting to the endoplasmic reticulum (ER), an N-terminal Flag epitope tag (YKDDDDK), and a C-terminal hexahistidine tag.<sup>24</sup> The plasmids were transformed by electroporation into the *Saccharomyces cerevisiae* strain YVH10, modified from the yeast strain BJ $\alpha$ 5464 to overexpress protein disulfide isomerase under control of the constitutive glyceraldehyde-3-phosphate dehydrogenase promoter.<sup>24,33</sup> The transformants were grown in 1 L of selective SD-SCAA + Trp (20 mg/L) media at 30°C to an  $\text{OD}_{600}$  of 6, and were pelleted by centrifugation and resuspended in 1 L of SG-SCAA + Trp (20 mg/L) to induce protein expression. Lysozyme (Sigma) (1mg/mL) was added as a carrier protein to prevent secreted EGFR-ECD protein from nonspecifically adhering to the flask walls, and the cultures were grown at 30°C under inducing conditions for 48 h. The N-terminal Flag epitope tagged sEGFR-ECDs were purified by immunoaffinity chromatography using anti-Flag M2 antibody agarose resin (Sigma) follow-

ing the manufacturer's instructions. The purified samples were analyzed by SDS-PAGE (4–12% Bis-Tris gel) (Invitrogen) under reducing and nonreducing conditions and were typically found to have greater than 95% purity. Treatment of the sEGFR-ECDs with endoglycosidase PNGase F (New England Biolabs) was performed in native or denatured conditions according to the manufacturer's instructions. The protein concentrations of sEGFR-ECDs were determined by UV-Vis spectrophotometry (Varian) using an extinction coefficient of  $55,900 \text{ M}^{-1}\text{cm}^{-1}$  at 280 nm.<sup>12</sup> The ligand binding affinities of the sEGFR-ECDs were measured with hEGF expressed on the yeast cell surface, in the pCTCON display vector. Yeast cells ( $10^6$ ) displaying hEGF were incubated with various concentrations of sEGFR-ECDs at 25°C with gentle agitation for 1 h. The bound sEGFR-ECDs were detected by incubation with biotinylated anti-FLAG M2 antibody, followed by addition of streptavidin-PE and analysis by flow cytometry. The mean fluorescence intensity was normalized by maximal and minimal mean fluorescence intensities to obtain the fraction of sEGFR-ECD binding to the surface displayed hEGF. Assuming a single site binding model with no ligand depletion, the apparent  $K_D$  values were obtained by fitting the data using the equation for the single site binding model.<sup>23,31</sup>

### Biological Assays in Mammalian Cells

The open reading frame of human EGFR was subcloned into pcDNA3 (Invitrogen) using *Xho*I and *Xba*I restriction sites, generating the expression vector pcDNA-EGFR. The pcDNA-EGFR contains a Kozak translation initiation sequence and the native N-terminal signal peptide sequence. *Nhe*I and *Age*I restriction sites were silently introduced at the N- and C-terminal regions of the EGFR-ECD, respectively, to easily subclone mutant EGFR-ECDs in-frame into the pcDNA-EGFR. A Chinese hamster ovary (CHO) K1 cell line was maintained in DMEM supplemented with 10 % (v/v) fetal bovine serum, 4 mM L-glutamine, 1 mM sodium pyruvate and 1 % (v/v) 100x non-essential amino acids for 48 h.<sup>6,34</sup> The expression plasmids were transiently transfected into the CHO cells using FuGene6 (Roche), following the manufacturer's protocol. After 2 d, cells were starved in serum free media for 12 h, and stimulated for 5 min with 25 nM hEGF.<sup>6</sup> Equivalent amounts of whole cell lysates were analyzed by SDS-PAGE and subsequent immunoblotting with rabbit polyclonal anti-human EGFR 1005 and rabbit polyclonal anti-human phospho-EGFR antibody Tyr 1173 (Santa Cruz Biotechnology), and polyclonal anti-MAP kinase antibody and anti-phospho-p44/42 MAP kinase E10 mAb (Cell Signaling Technology). Blots were incubated with horseradish peroxidase-conjugated anti-mouse IgG antibody (Sigma), and developed using enhanced chemiluminescence with ECL plus western blotting detection reagents (Amersham Biosciences).

### Full-Length EGFR Expression in Yeast

Full-length wild type and mutant EGFR from pcDNA-EGFR plasmids were subcloned into pRS GAL for the



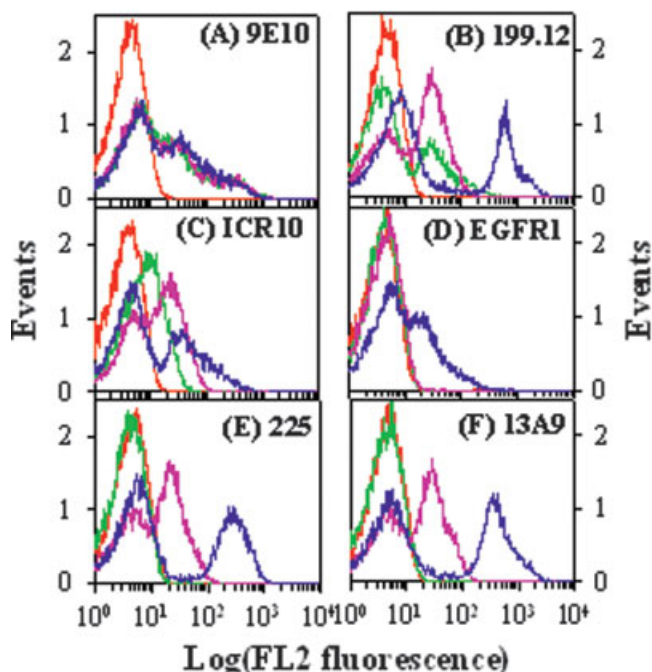


Fig. 1. Flow cytometric analysis of indirect immunofluorescence (i.e., primary labeling by EGFR-ECD specific mAb and subsequent secondary labeling with goat anti-mouse-PE secondary antibody) of yeast (pCaga2 based display plasmid) expressing the EGFR-ECD wild type (green), dm mutant (pink), and 404SG mutant (blue), and negative control (red). **A:** The expression levels of EGFR-ECD was measured using the anti-c-myc mAb 9E10. Proper protein folding was assessed by reactivity with conformation-specific mAbs 199.12 (**B**), ICR10 (**C**), EGFR1 (**D**), 225 (**E**), and 13A9 (**F**).

expression in the yeast strain YVH10.<sup>33</sup> Cultures were grown in SD-SCAA + Trp media at 30°C to an OD<sub>600</sub> of 5. Yeast cells (10<sup>7</sup>) were pelleted by centrifugation, and transferred into SG-SCAA + Trp induction media, and grown for an additional 6 h. Spheroplasts were prepared by zymolase treatment (Zymo Research) according the manufacturer's instructions in PBSB buffer containing 1.2 M sorbitol, 2× protease inhibitor cocktail (P8215, Sigma), and 1 mM PMSF.<sup>35</sup> After preparation of spheroplasts, primary and secondary antibody labelings were performed in PBSB with 1.2 M sorbitol.<sup>35</sup> Samples were analyzed by flow cytometry and fluorescence microscopy using a Delta-Vision deconvolution microscope with an 100× oil objective (Applied Precision).<sup>35</sup>

## RESULTS

### Expression of the EGFR-ECD on the Yeast Cell Surface

The EGFR-ECD (residues 1–621) was expressed on the yeast cell surface as an N- or C-terminal fusion to the agglutinin binding subunit Aga2p. EGFR-ECD expression levels were determined by indirect immunofluorescence of a C-terminal c-myc epitope tag using flow cytometry.<sup>29</sup> Flow cytometric histograms always showed background auto fluorescence with intensity below 10 by cells not expressing EGFR-ECD (Fig. 1), which is a typical phenomenon of yeast display system and likely to be caused by



Fig. 2. X-ray crystallographic structure of the EGFR-ECD (PDB accession code 1NQL).<sup>4</sup> The program Rasmol was used to highlight the mutated residues as space-filling models (gray), and color the receptor subdomains: domain I (green), domain II (magenta), domain III (green-blue), and domain IV (pink).

plasmid loss during culturing.<sup>18,19,24,29</sup> Significant positive labeling of the c-myc epitope tag demonstrated the expression of EGFR-ECD on the yeast cell surface [Fig. 1(A)]. N-Aga2p-fused EGFR-ECD showed slightly higher levels of c-myc labeling, but similar levels of labeling of conformation-specific mAbs against EGFR-ECD, compared with that of C-Aga2p-fused EGFR-ECD (data not shown), indicative of negligible topology effects on the accessibility of the anti-c-myc specific mAb. The protein expression levels were higher at induction temperatures of 20 and 30°C, than at 37°C, independent of the length of induction time between 16 to 48 h (data not shown).

To determine whether the wt EGFR-ECD was properly folded on the yeast-cell surface, conformation-specific mAbs against the EGFR-ECD were employed for the flow cytometry analysis (Fig. 1). Our recent epitope mapping studies using yeast surface displayed EGFR-ECD fragments demonstrated that mAbs 199.12, ICR10, EGFR1, 225, and 528 recognize conformational or discontinuous EGFR epitopes.<sup>23</sup> The epitopes of mAbs ICR10 and 199.12 are between EGFR residues 124–176 (Domain I), and the epitope of mAb EGFR1 is between EGFR residues 176–294 (Domain II).<sup>23</sup> The epitopes of mAbs 225, 528 and 13A9 lie between EGFR residues 294–543 (Domain III),<sup>23,36</sup> which is consistent with the EGFR expressed in mammalian cells.<sup>37,38</sup> The wt EGFR-ECD expressed on the surface of yeast showed weak binding for the EGFR conformation-specific mAbs 199.12 and ICR10 (Fig. 1). Conformation-specific mAbs EGFR1, 225, 528, and 13A9 did not bind to the yeast surface-displayed EGFR-ECD, indicative of the lack of conformational epitopes in the EGFR domains II and III. We cannot determine the conformation of the yeast-displayed EGFR domain IV due to the lack of conformation-specific mAbs against this region, but the mAb 2D2 raised against the linear epitope 556–567<sup>39</sup> bound well to the yeast expressed EGFR-ECD.<sup>23</sup> The binding profiles of the mAbs against the EGFR-ECD were

independent of the N-Aga2 and C-Aga2 fused forms, overexpression of protein disulfide isomerase, induction temperature (20, 30, and 37°C), and induction time (16–48 hours) (data not shown). Taken together, this data demonstrates that the EGFR-ECD is well expressed on the yeast cell surface, and yet it is partially misfolded, particularly in domains II and III.

### Screening of EGFR-ECD Mutants

Directed evolution and yeast surface display were used to isolate EGFR-ECD mutants with proper folding, using the conformation-specific mAbs 199.12, 225, 528, and EGFR1 as screening probes. The ligand EGF was not used as a screening probe because fluorescently labeled EGF, Alexa 488-EGF, exhibited nonspecific labeling to yeast cell surfaces at micromolar concentrations. A mutagenic EGFR-ECD library of  $10^8$  transformants was constructed by error prone PCR and expressed on the surface of yeast. The library was screened by fluorescence-activated cell sorting (FACS), with alternating immunofluorescent labelings using mAbs 225, 528, and 199.12. Yeast cells were subjected to six rounds of FACS, with regrowth and induction of cells in between sorts. The top 1–2 % fluorescent cells were selected for isolation in each round of sorting to obtain an enriched population of EGFR-ECD mutants that were recognized by the conformationally-specific mAbs. Plasmid DNA was rescued from individual yeast clones, and the amino acid sequences of 12 unique mutants were determined. DNA sequencing identified deletion mutants, and 1–4 amino acid mutations throughout the EGFR-ECD, with the mutations F380S and S418G in domain III occurring frequently. Using site-directed mutagenesis, an EGFR-ECD mutant (designated “dm”) was constructed, possessing only the F380S and S418G mutations. The dm mutant showed similar yeast surface expression levels to that of wild type EGFR-ECD based on anti-c-myc 9E10 labeling, but exhibited increased binding to the domain I conformation-specific mAbs 199.12 and ICR10, and strong binding to the domain III conformation-specific mAbs 225, 528, and 13A9 (Fig. 1). However, the dm mutant still did not bind to the domain II conformation-specific mAb EGFR1 [Fig. 1(D)]. Thus, the dm mutant appears to be properly folded in domain III compared with the wild type EGFR-ECD, but is still misfolded in the domain II region of the receptor.

To isolate mutants that bind to mAb EGFR1, another round of EGFR-ECD engineering was performed using mAbs EGFR.1 and 225 as screening probes. The mAb 225 was used to retain the beneficial mutations of F380S and S418G in domain III while screening mutants with proper folding of domain II by the mAb EGFR1. A mutagenic EGFR-ECD library of  $10^8$  transformants was constructed by the combination of error prone PCR and DNA shuffling using the pCaga2 display plasmid templates of wild type (20%), the dm mutant (40%), and an aglyco mutant (40%), “N(12)A,” which has all mutations of Asn to Ala at the potential 12 glycosylation sites.<sup>28</sup> In this library, the pCaga2 plasmid was used to tether the EGFR-ECD to the yeast cell surface by the protein C-terminus, and leave a

free N-terminus, like the natural receptor state in mammalian cells. Sequence analysis of the EGFR-ECD showed 12 potential N-glycosylation sites (N-X-S/T, X can be any amino acid except proline) without O-linked glycosylation.<sup>3,28</sup> The N(12)A mutant was not displayed on the yeast cell surface (data not shown), however N(12)A DNA was added into the library shuffling reactions in an attempt to isolate properly folded mutants with minimal glycosylation. Sequencing of eight plasmids from the original library showed a diverse range of mutagenic frequencies, from 2–14 amino acid changes in the EGFR-ECD, with an average of six mutations. Ten cycles of flow cytometric sorting were performed, alternating the labeling of the cells with mAbs 225 and EGFR.1. Isolation and sequencing of 14 clones identified only two unique mutants, designated clones 38-7 and 40-4. The sequence analysis showed total mutation rate of about 0.3 % at the nucleotide level, with 0.14 % sense and 0.16% nonsense, and 0.19% transition and 0.11% transversion mutations. Clone 38-7 has mutations Q59R and L69H, and clone 40-4 has mutations A62T, L69H, and G161S. In addition, both clones retained the two mutations F380S and S418G found in the original dm mutant. Interestingly, no Asn to Ala glycosylation mutations were enriched during the library screens. When the mutants were characterized for mAb binding, clone 40-4 showed much better binding than clone 38-7 to the conformation-specific mAbs 225, 528, 13A9, and EGFR. However, clone 40-4 did not bind to the mAb 199.12. To parse the amino acid residues responsible for the differential mAb reactivity, site-directed mutagenesis was used to construct all possible mutants with combinations of single or double mutations of Q59R, A62T, L69H, while retaining F380S and S418G. Characterization of these mutant EGFR-ECDs by mAb labeling demonstrated that the G161S mutation is responsible for the disappearance of mAb 199.12 binding epitope, and Q59R is unessential for the binding to all mAbs tested (data not shown). Thus we constructed one mutant with A62T, L69H, F380S, and S418G, designated the 404SG mutant (Fig. 2). While 404SG showed similar expression levels on the yeast cell surface compared to wild type and the dm mutant, it demonstrated increased reactivity to all tested conformation-specific mAbs (Fig. 1).

### hEGF Binding and Thermal Stability of EGFR-ECDs

The binding affinity of hEGF for the wild type and mutant EGFR-ECDs displayed on the yeast cell surface was determined by competition binding with the mAb 225. The mAb 225 is known to efficiently compete with hEGF for binding to EGFR expressed on mammalian cells.<sup>38</sup> The apparent  $K_D$  value of mAb 225 for the yeast displayed EGFR-ECD was determined to be  $0.48 \pm 0.05$  nM for both the dm and the 404SG mutants (data not shown). This is consistent with the previously reported values for mAb 225 binding to EGFR expressed in A431 carcinoma cells (~1 nM), HeLa cells (1.1 nM), and human fibroblasts (1 nM).<sup>38</sup> Therefore, mutations that were selected during the library screening do not confer higher binding affinity to

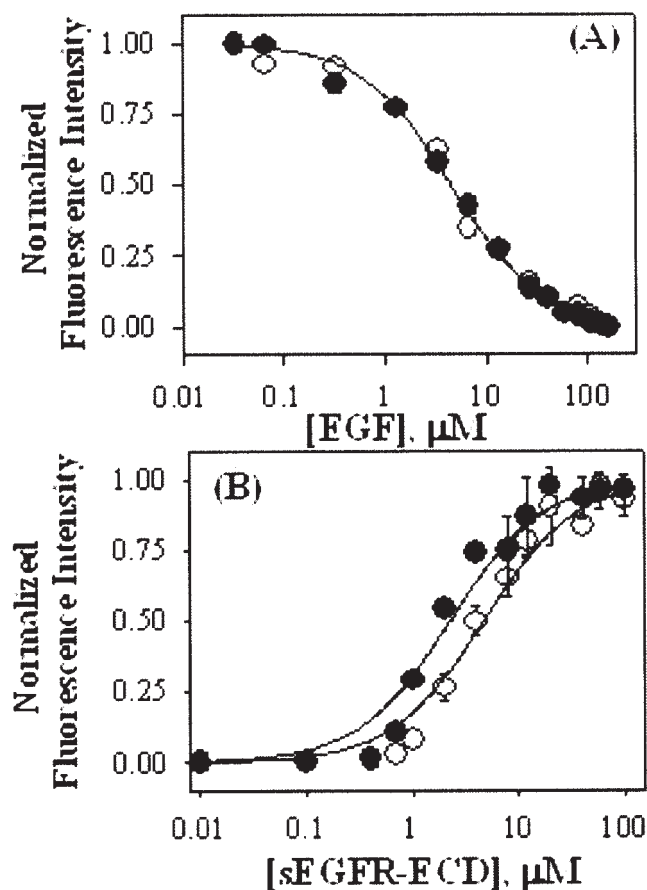


Fig. 3. hEGF binding to mutant EGFR-ECDs. **A:** Competition assay of hEGF with mAb 225 for binding to the dm mutant ( $\circ$ ) and the 404SG mutant ( $\bullet$ ) expressed on the yeast cell surface. **B:** Binding assay of the soluble dm mutant ( $\circ$ ) and the 404SG mutant ( $\bullet$ ) to hEGF expressed on the yeast cell surface. Error bars indicate the standard deviation for duplicate samples.

the mAb 225. Instead, the 404SG mutant showed a higher relative maximum fluorescence intensity than the dm mutant, indicative of conformational differences between the two proteins. An apparent hEGF  $K_D$  value of  $0.87 \pm 0.08 \mu\text{M}$  for both the dm and 404SG mutants expressed on yeast was obtained by competition binding of mAb 225 with hEGF (Fig. 3), assuming competition of hEGF with mAb225 for a single binding site of EGFR-ECD,<sup>38</sup> the same expression level of dm and 404SG on the cell surface, and no ligand depletion. These values are consistent with what has previously been seen with soluble hEGF binding to soluble EGFR-ECD expressed in insect and mammalian cells ( $K_D = 0.1\text{--}0.5 \mu\text{M}$ ).<sup>12,40</sup> However, these values are much lower than those for full-length EGFR expressed on mammalian cell surfaces, which binds to hEGF with low affinity ( $K_D = 1\text{--}2 \text{ nM}$ ) and high affinity ( $K_D = 10\text{--}50 \text{ pM}$ ) sites.<sup>41</sup> These differences are most likely due to the inability of yeast-displayed EGFR-ECD to dimerize upon ligand binding, due to constraints in the rigid cell wall. It has been shown that EGFR mutants that lack dimerizing determinants in domain II have significantly decreased ligand binding affinity.<sup>6</sup> The hEGF also competed with the

mAb 528, but did not compete with the mAb 13A9 for the binding to both the dm and 404SG mutants (data not shown), consistent with previous results in EGFR-expressing mammalian cells.<sup>38,42</sup> The relative thermal stability of wild type EGFR-ECD, and the dm and 404SG mutants was directly compared on the yeast cell surface<sup>32</sup> by the mAbs 199.12 and 225 using indirect immunofluorescence and flow cytometry. The order of apparent thermal stability of domain I was 404SG ( $61.0 \pm 1.3^\circ\text{C}$ ) > dm ( $55.6 \pm 0.8^\circ\text{C}$ ) > wild type ( $52.5 \pm 0.7^\circ\text{C}$ ) (data not shown). There was no difference in the relative thermal stability of domain III for the dm ( $58.5 \pm 1.1^\circ\text{C}$ ) and 404SG ( $57.8 \pm 0.6^\circ\text{C}$ ) (data not shown). For wild type, the thermal stability of domain III could not be measured due to its inability to bind to the conformation-specific mAb 225.

### Soluble Production of EGFR-ECDs

To compare the EGFR-ECD protein expression efficiency, wild type, and the dm and 404SG mutants were expressed in soluble form with N-terminal Flag and C-terminal His<sub>6</sub> epitope tags. The yeast strain YVH10, which overexpresses protein disulfide bond isomerase, was used to assist in the formation of the 25 disulfide bonds of the EGFR-ECD. Secretion efficiency of the 404SG mutant (typically 4–6 mg/L) was two to threefold higher than that of the dm mutant, which in turn was about twofold higher than that of wild type. Purified proteins were analyzed by reducing and nonreducing SDS-PAGE with or without endoglycosidase PNGase F treatment under native conditions (Fig. 4). PNGase F treatment removes protein N-glycosylation, including the terminal GlcNAc on Asn residues. Untreated sEGFR-ECDs exhibited heterogeneous smear bands with much a higher molecular weight than the theoretical molecular weight ( $\sim 70 \text{ kDa}$ ). With PNGase F treatment, the sEGFR-ECDs migration was consistent with a molecular mass of about 70 kDa, the predicted size of deglycosylated sEGFR-ECDs, under reducing conditions. Thus the heterogeneous smear bands are caused by hyperglycosylation of the EGFR proteins. Glycosylation of EGFR expressed in mammalian cells contributes an apparent 40 kDa of the mass to the mature protein.<sup>43</sup> Samples treated with PNGase F under native conditions still exhibited some smear bands, which disappeared when the samples were first denatured before PNGase F treatment (data not shown), suggesting that PNGase F cannot access all the glycosylation sites of this protein in the native state. Under nonreducing conditions, wild type EGFR-ECD did not show a single band, but broad heterogeneous bands even after the PNGase F treatment (Fig. 4), indicative of nonnative intermolecular disulfide-bonded linked oligomers or protein aggregates. In contrast, the dm and 404SG mutants exhibited a single band around a molecular weight of 70 kDa, suggesting that they were expressed as monomeric species. It should be noted that the 404SG mutant exhibited a homogeneously glycosylated band around 120 kDa even without PNGase F treatment in addition to the heterogeneous smear bands in both reducing and nonreducing conditions.



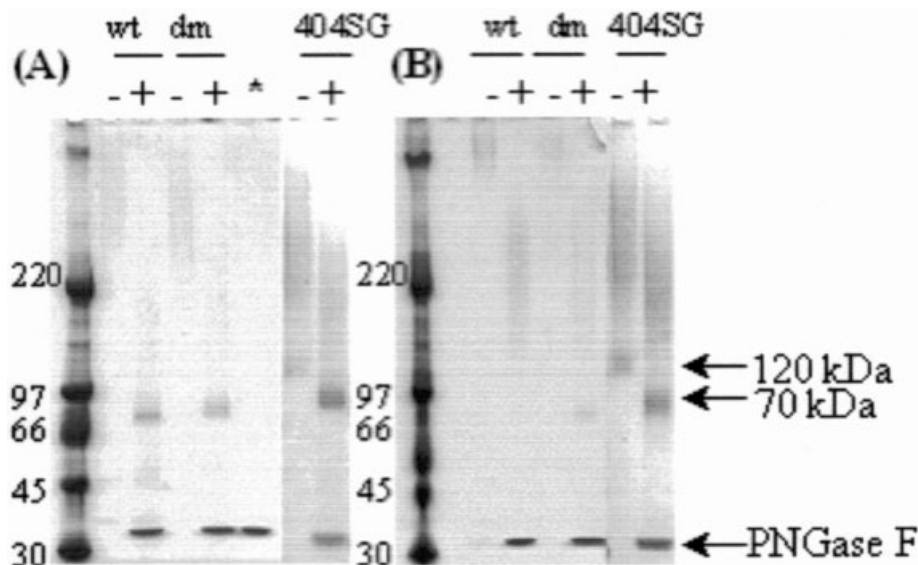


Fig. 4. Reducing (A) and nonreducing (B) SDS-PAGE of sEGFR-ECDs produced from the *S. cerevisiae* strain YVH10. Samples were analyzed after treatment with (+) or without (–) endoglycosidase PNGase F under native conditions. The gel (4–12% Bis-Tris) was stained with Coomassie brilliant blue. The deglycosylated EGFR-ECD (~70 kDa), homogeneously glycosylated 404SG (~120 kDa), and PNGase F (~36 kDa) are indicated by arrows. \* indicates the control lane loaded with only PNGase F.

Ligand binding affinities for the sEGFR-ECDs were estimated using hEGF displayed on the yeast-cell surface [Fig. 3(B)]. Wild type sEGFR-ECD did not show any binding to yeast-displayed hEGF up to a 50  $\mu$ M protein concentration tested. Consistent with the yeast-cell surface displayed EGFR-ECD, however, the soluble EGFR-ECD dm and 404SG mutants showed specific binding to hEGF with apparent  $K_D$  values of  $4.7 \pm 0.6$  and  $2.3 \pm 0.3$   $\mu$ M, respectively. Those values are somewhat lower than that of sEGFR-ECD ( $K_D = 0.1\text{--}0.5$   $\mu$ M) expressed in mammalian and insect cells.<sup>12,40</sup> Heterogeneous populations of sEGFR-ECDs due to protein hyperglycosylation may be responsible for the weaker binding affinity to hEGF. Based on this hypothesis, the approximately two-fold higher affinity of the soluble 404SG mutant to hEGF may be attributed to the homogeneous population present in soluble form, compared with the soluble dm mutant (Fig. 4).

#### Biological Assays of the Mutant EGFR-ECDs in Mammalian Cells

To address whether the mutant EGFR-ECDs engineered in yeast are biologically functional in mammalian cells, full-length EGFR (including the transmembrane and cytoplasmic domains) with the dm and 404SG mutant EGFR-ECDs were transfected into CHO cells to assay for intrinsic functions such as expression, activation by autophosphorylation, and intracellular signaling. The CHO K1 cells do not express endogenous EGFR.<sup>6,34</sup> Full-length dm and 404SG EGFR were expressed at similar cell surface levels as wild type EGFR (not shown), and exhibited robust autophosphorylation in response to hEGF stimulation [Fig. 5(A)]. Flow cytometric analysis of the EGFR on the CHO cell surface by mAbs 199.12, 225, and EGFR1 did

not show any significant differences in the magnitude of fluorescence intensity between wild type and the dm and 404SG mutants (data not shown). This suggests that on the surface of mammalian cells the wild type and mutant EGFR-ECD proteins have similar conformational epitopes, unlike what is seen on the yeast cell surface. A consequence of ligand-induced stimulation of EGFR is the activation of the extracellular signal-regulated protein kinases (ERK) cascade, including p42/p44 MAP kinase.<sup>1,2</sup> The activation of full-length dm and 404SG EGFR mutants induced the activation of MAPK p42/p44 at similar levels with wild type EGFR [Fig. 5(B)]. These results suggest that full-length dm and 404SG EGFR mutants are functional and indistinguishable from the wild type EGFR in terms of cell surface expression and activation of intracellular signaling in mammalian cells.

#### Full-Length EGFR Expression in Yeast

We investigated whether the full-length EGFR could be expressed in the plasma membrane of yeast in its properly folded form. DNA encoding for the wild type and the 404SG mutant EGFR-ECD, and including the EGFR transmembrane and cytoplasmic domains, were transformed into the yeast strain YVH10. After induction of the full-length EGFRs at 30°C for 6 h, spheroplasts were prepared to remove the yeast cell wall. Spheroplasts were labeled by the anti-Flag mAb M2 to detect the N-terminal Flag epitope or the EGFR-specific mAbs 199.12 and 225, and were analyzed by flow cytometry or immunofluorescence microscopy (Fig. 6). Both the full-length wild type and the 404SG mutant EGFRs showed positive labeling by the mAbs M2 and 199.12, demonstrating their expression and localization at the plasma membrane. The higher fluorescence intensity of the Flag epitope tag labeling for

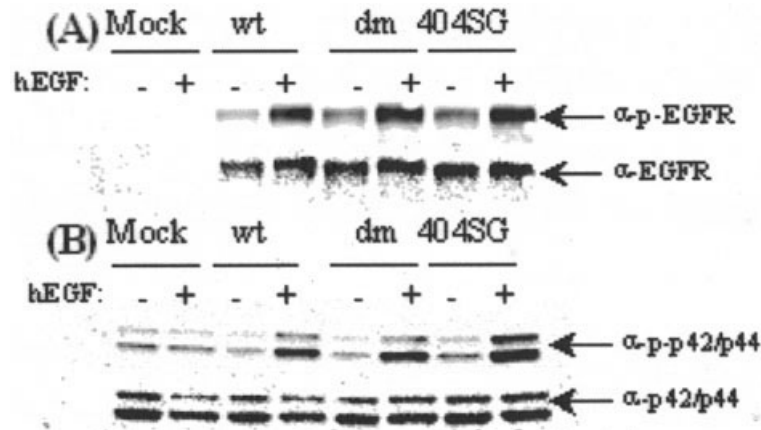


Fig. 5. hEGF-induced EGFR activation and ERK signaling in CHO cells transiently transfected with full-length wild type, dm, and 404SG EGFRs. Transfected cells were treated with (+) or without (–) 25 nM hEGF for 5 min, and equivalent amounts of whole cell lysates were analyzed by SDS-PAGE followed by immunoblotting. (A) EGF-induced autophosphorylation of EGFR was monitored by probing the blot with anti-phospho-EGFR (α-p-EGFR) (upper panel). Blots were stripped and re-probed with anti-EGFR (α-EGFR) (lower panel) to determine total EGFR levels. (B) EGF-induced ERK phosphorylation was monitored by probing the blots with anti-phospho-p42/p44 (α-p-p42/p44) (upper panel). Blots were stripped and re-probed with anti-p42/p44 (α-p42/p44) (lower panel) to determine total ERK levels.

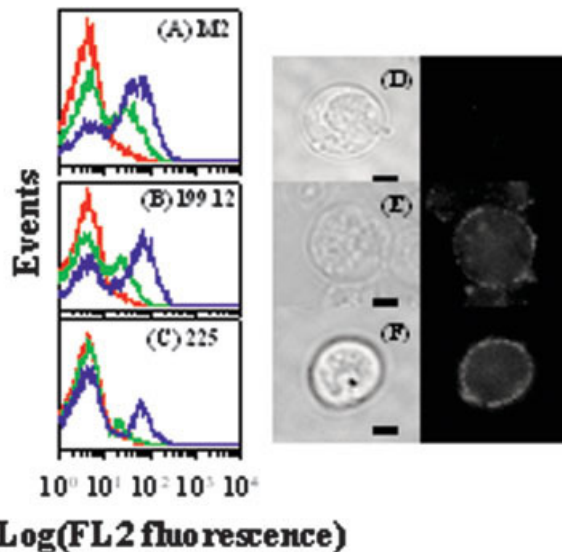


Fig. 6. Expression and localization of full-length wild type and 404SG EGFR in the yeast strain YVH10. Spheroplast preparations of yeast cells expressing full-length wild type EGFR (green), 404SG EGFR (blue), and a mock plasmid negative control (red), were labeled with anti-Flag mAb M2 (A) and anti-EGFR mAbs 199.12 (B) and 225 (C), and analyzed by flow cytometry. The spheroplast cells labeled with mAb 199.12 were also analyzed by fluorescence microscopy for expression of mock plasmid (D), wild type EGFR (E), and 404SG EGFR (F), where the left and right panels show the phase contrast and fluorescence images, respectively. Scale bars indicate 1 μm.

the full-length 404SG EGFR indicates its increased expression level at the plasma membrane relative to the wild type EGFR. Like the EGFR-ECDs displayed on the yeast-cell surface, mAb 199.12 bound more efficiently and mAb 225 only bound to full-length 404SG mutant EGFR, compared with wild type. These observations demonstrate

that the conformations of the ECDs of full-length EGFR expressed at the plasma membrane are comparable to those of EGFR-ECDs alone on the yeast cell surface (Figs. 1,6).

## DISCUSSION

Wild type EGFR-ECD was expressed in *Saccharomyces cerevisiae*, but in a partially misfolded state that when secreted formed non-native intermolecular disulfide bonds and large aggregates. Not surprisingly, this protein in its secreted form showed no binding to the hEGF ligand. Given the quality control system of the yeast secretory pathway, believed to allow export of only properly folded proteins,<sup>13,14,44</sup> it was somewhat unexpected to find significant quantities of misfolded EGFR-ECD on the yeast cell surface. Previous studies have shown that T cell receptors and class II major histocompatibility proteins were not expressed on the yeast cell surface until engineering studies identified mutations which increased thermal stability and induced proper protein folding.<sup>19,21</sup> The EGFR-ECD's misfolded conformation is apparently not recognized by the yeast quality control system, allowing for its efficient secretion and export to the cell surface. The mutant EGFR-ECDs showed higher thermal stability and secretion efficiency compared to wild type protein, consistent with previous observations of a direct relationship between secretion efficiency and thermodynamic stability of proteins expressed in *Saccharomyces cerevisiae*.<sup>18,19,24,44</sup>

Two rounds of directed evolution and screening on the yeast cell surface identified 404SG, a mutant EGFR-ECD with proper folding and functionality. The two mutations F380S and S418G in domain III of the dm and 404SG mutants allowed for conformational reactivity of the domain III mAbs 225, 528, and 13A9. The fact that mAb 225 competes with hEGF for the binding to the EGFR-ECD indicates that they recognize same local tertiary conforma-



tions. The F380S and S418G mutations are close to interfacial interactions between domain III of EGFR and hEGF,<sup>6</sup> indicating that these mutations induce the proper conformation for binding of the mAb225 and hEGF. Furthermore, these two mutations might not only affect local conformations around the mAb 225 binding epitope, but might also induce global conformational changes in domain III. EGFR-ECD proteins containing the F380S and S418G mutations confer binding of the mAb 13A9, which like the EGFR present in mammalian cells, does not compete with hEGF binding.<sup>38,42</sup> The mutations A62T and L69H in domain I of the 404SG mutant induced reactivity of domain II against the conformation-specific mAb EGFR1, and increased binding to all of the other mAbs and hEGF to the EGFR-ECD (Figs. 1–3). Interestingly, the mutations F380S and S418G in domain III contributed to higher thermal stability of domain I. Recent structural data showed that domain I and III are separated by domain II without any domain-to-domain interactions.<sup>4,6</sup> This suggests that the four mutations identified from our studies are not involved in domain-to-domain interactions (Fig. 2), and appear to be cooperative and additive, affecting subtle global conformations of the EGFR across the extracellular domain. Protein sequence analysis showed that all four mutations were present in the native sequences of other ErbB receptor family members and EGFR from other species (data not shown). The structure and function of EGFR is evolutionarily conserved from *Caenorhabditis elegans* to *Homo sapiens*.<sup>1,3</sup> Mutations that are biased toward homologous substitutions appear to be selected for maintaining protein integrity and stability, consistent with other directed evolution studies in our laboratory, (J.R.C., B.R., Y.S.K., and K.D.W., manuscript in preparation).

Glycosylation is a frequent posttranslational modification in extracellular eukaryotic proteins, influencing a wide range of protein structure and functions, such as folding, secretion, and stability.<sup>13,14</sup> Unlike mammalian cells, N-glycosylation in yeast involves the addition of high numbers of mannose moieties (> 100 mannoses) during trafficking in the Golgi to the core oligosaccharide chains formed in the endoplasmic reticulum,<sup>13,14</sup> which is one of the main limitations of the heterologous expression of glycoproteins in yeast. Without any mutations at the potential N-linked glycosylation sites, the 404SG EGFR-ECD mutant was solubly expressed in a partially homogeneously glycosylated form, indicating that the residence time of the protein in the Golgi is relatively short compared with the wild type and the dm mutant. Such homogeneity of a yeast-expressed mammalian glycoprotein has also been observed with single chain T cell receptor mutants with higher thermal stability.<sup>24</sup> Perhaps improved thermal stability and proper folding of proteins can avoid the rerouting process from the Golgi to the endoplasmic reticulum for misfolded proteins, shortening the residency time in the Golgi and consequently reducing hypermannosylation.

The full-length EGFR mutants were well expressed and functional in the mammalian cell model system. There-

fore, the full-length EGFR mutants are correctly processed and folded in the mammalian endoplasmic reticulum. This result further supports the goal of engineering mammalian membrane glycoproteins in yeast. The full-length 404SG EGFR was also expressed in a properly folded form and localized at the plasma membrane in yeast, allowing for future structural and functional studies of full-length EGFR in yeast (Fig. 6).

These studies demonstrate that directed evolution of the EGFR-ECD leads to functional expression in soluble form, and full-length EGFR expression at the plasma membrane of yeast. The expression of complicated mammalian membrane proteins is essential for their structural and functional characterization, but often involves significant challenges in order to achieve homogeneous production. Our study provides an example of the functional expression of a complex mammalian membrane protein in a system amenable to facile genetics and culture. Large quantities of this modified soluble EGFR-ECD protein can be produced for the screening of receptor agonists or antagonists, and for biophysical studies.

## ACKNOWLEDGMENTS

We thank Dr. Nita J. Mairle of the Mayo Cancer Center for the generous gift of the mAb 2D2, John Albeck of Department of Biology at MIT for assistance with fluorescence microscopy, Dr. Xuewu Zhang in the Kuriyan group and the Wittrup group members for helpful discussions. This work was supported by CA96504.

## REFERENCES

1. Jorissen RN, Walker F, Pouliot N, Garrett TP, Ward CW, Burgess AW. Epidermal growth factor receptor: mechanisms of activation and signalling. *Exp Cell Res* 2003;284:31–53.
2. Yarden Y. The EGFR family and its ligands in human cancer. Signalling mechanisms and therapeutic opportunities. *Eur J Cancer* 2001;37 Suppl 4:S3–S8.
3. Ullrich A, Coussens L, Hayflick JS, Dull TJ, Gray A, Tam AW, Lee J, Yarden Y, Libermann TA, Schlessinger J, et al. Human epidermal growth factor receptor cDNA sequence and aberrant expression of the amplified gene in A431 epidermoid carcinoma cells. *Nature* 1984;309: 418–425.
4. Ferguson KM, Berger MB, Mendrola JM, Cho HS, Leahy DJ, Lemmon MA. EGF activates its receptor by removing interactions that autoinhibit ectodomain dimerization. *Mol Cell* 2003;11:507–517.
5. Garrett TP, McKern NM, Lou M, Elleman TC, Adams TE, Lovrecz GO, Zhu HJ, Walker F, Frenkel MJ, Hoyne PA, Jorissen RN, Nice EC, Burgess AW, Ward CW. Crystal structure of a truncated epidermal growth factor receptor extracellular domain bound to transforming growth factor alpha. *Cell* 2002;110:763–773.
6. Ogiso H, Ishitani R, Nureki O, Fukai S, Yamanaka M, Kim JH, Saito K, Sakamoto A, Inoue M, Shirouzu M, Yokoyama S. Crystal structure of the complex of human epidermal growth factor and receptor extracellular domains. *Cell* 2002;110:775–787.
7. Burgess AW, Cho HS, Eigenbrot C, Ferguson KM, Garrett TP, Leahy DJ, Lemmon MA, Sliwkowski MX, Ward CW, Yokoyama S. An open-and-shut case? Recent insights into the activation of EGF/ErbB receptors. *Mol Cell* 2003;12:541–552.
8. Ciardiello F, Tortora G. Epidermal growth factor receptor (EGFR) as a target in cancer therapy: understanding the role of receptor expression and other molecular determinants that could influence the response to anti-EGFR drugs. *Eur J Cancer* 2003;39:1348–1354.
9. Arteaga CL. ErbB-targeted therapeutic approaches in human cancer. *Exp Cell Res* 2003;284:122–130.
10. Berezov A, Chen J, Liu Q, Zhang HT, Greene MI, Murali R.

- Disabling receptor ensembles with rationally designed interface peptidomimetics. *J Biol Chem*, 2002;277:28330–28339.
11. Ferguson KM, Darling PJ, Mohan MJ, Macatee TL, Lemmon MA. Extracellular domains drive homo- but not hetero-dimerization of erbB receptors. *Embo J* 2000;19:4632–4643.
  12. Lemmon MA, Bu Z, Ladbury JE, Zhou M, Pinchasi D, Lax I, Engelman DM, Schlessinger J. Two EGF molecules contribute additively to stabilization of the EGFR dimer. *Embo J* 1997;16:281–294.
  13. Ellgaard L, Helenius A. Quality control in the endoplasmic reticulum. *Nat Rev Mol Cell Biol* 2003;4:181–191.
  14. Eckart MR, Bussineau CM. Quality and authenticity of heterologous proteins synthesized in yeast. *Curr Opin Biotechnol* 1996;7:525–530.
  15. Wittrup KD. Protein engineering by cell-surface display. *Curr Opin Biotechnol* 2001;12:395–399.
  16. Vasserot AP, Dickinson CD, Tang Y, Huse WD, Manchester KS, Watkins JD. Optimization of protein therapeutics by directed evolutions. *Drug Discov Today* 2003;8:118–126.
  17. Boder ET, Midelfort KS, Wittrup KD. Directed evolution of antibody fragments with monovalent femtomolar antigen-binding affinity. *Proc Natl Acad Sci USA* 2000;97:10701–10705.
  18. Shusta EV, Holler PD, Kieke MC, Kranz DM, Wittrup KD. Directed evolution of a stable scaffold for T-cell receptor engineering. *Nat Biotechnol* 2000;18:754–759.
  19. Kieke MC, Shusta EV, Boder ET, Teyton L, Wittrup KD, Kranz DM. Selection of functional T cell receptor mutants from a yeast surface-display library. *Proc Natl Acad Sci USA* 1999;96:5651–5656.
  20. Schweickhardt RL, Jiang X, Garone LM, Brondyk WH. Structure-expression relationship of tumor necrosis factor receptor mutants that increase expression. *J Biol Chem* 2003;278:28961–28967.
  21. Starwalt SE, Masteller EL, Bluestone JA, Kranz DM. Directed evolution of a single-chain class II MHC product by yeast display. *Protein Eng* 2003;16:147–56.
  22. Zhan H, Liu B, Reid SW, Aoki KH, Li C, Syed RS, Karkaria C, Koe G, Sitney K, Hayenga K, Mistry F, Savel L, Dreyer M, Katz BA, Schreurs J, Matthews DJ, Cheetham JC, Egrie J, Giebel LB, Stroud RM. Engineering a soluble extracellular erythropoietin receptor (EPObp) in *Pichia pastoris* to eliminate microheterogeneity, and its complex with erythropoietin. *Protein Eng* 1999;12:505–513.
  23. Cochran JR, Kim YS, Olsen MJ, Bhandari R, Wittrup KD. Domain-level antibody epitope mapping through yeast surface display of epidermal growth factor receptor fragments. *J Immunol Methods* 2004;287:147–158.
  24. Shusta EV, Kieke MC, Parke E, Kranz DM, Wittrup KD. Yeast polypeptide fusion surface display levels predict thermal stability and soluble secretion efficiency. *J Mol Biol* 1999;292:949–956.
  25. Zaccolo M, Williams DM, Brown DM, Gherardi E. An approach to random mutagenesis of DNA using mixtures of triphosphate derivatives of nucleoside analogues. *J Mol Biol* 1996;255:589–603.
  26. Stemmer WP. DNA shuffling by random fragmentation and reassembly: in vitro recombination for molecular evolution. *Proc Natl Acad Sci USA* 1994;91:10747–10751.
  27. Kim YS, Jung HC, Pan JG. Bacterial cell surface display of an enzyme library for selective screening of improved cellulase variants. *Appl Environ Microbiol* 2000;66:788–793.
  28. Zhen Y, Caprioli RM, Staros JV. Characterization of glycosylation sites of the epidermal growth factor receptor. *Biochemistry* 2003;42:5478–5492.
  29. Boder ET, Wittrup KD. Yeast surface display for screening combinatorial polypeptide libraries. *Nat Biotechnol* 1997;15:553–557.
  30. Swers JS, Kellogg BA, Wittrup KD. Shuffled antibody libraries created by in vivo homologous recombination and yeast surface display. *Nucleic Acids Res* 2004, forthcoming.
  31. Stein RA, Wilkinson JC, Guyer CA, Staros JV. An analytical approach to the measurement of equilibrium binding constants: application to EGF binding to EGF receptors in intact cells measured by flow cytometry. *Biochemistry* 2001;40:6142–6154.
  32. Orr BA, Carr LM, Wittrup KD, Roy EJ, Kranz DM. Rapid method for measuring ScFv thermal stability by yeast surface display. *Biotechnol Prog* 2003;19:631–638.
  33. Robinson AS, Hines V, Wittrup KD. Protein disulfide isomerase overexpression increases secretion of foreign proteins in *Saccharomyces cerevisiae*. *Biotechnology (N Y)* 1994;12:381–384.
  34. Kim JH, Saito K, Yokoyama S. Chimeric receptor analyses of the interactions of the ectodomains of ErbB-1 with epidermal growth factor and of those of ErbB-4 with neuregulin. *Eur J Biochem* 2002;269:2323–2329.
  35. Rines DR, He X, Sorger PK. Quantitative microscopy of green fluorescent protein-labeled yeast. *Methods Enzymol* 2002;351:16–34.
  36. Chao G, Cochran JR, Wittrup KD. Fine epitope mapping of anti-epidermal growth factor receptor antibodies through random mutagenesis and yeast surface display. *J Mol Biol* 2004;342:539–550.
  37. Gill GN, Kawamoto T, Cochet C, Le A, Sato JD, Masui H, McLeod C, Mendelsohn J. Monoclonal anti-epidermal growth factor receptor antibodies which are inhibitors of epidermal growth factor binding and antagonists of epidermal growth factor-stimulated tyrosine protein kinase activity. *J Biol Chem* 1984;259:7755–7760.
  38. Sato JD, Kawamoto T, Le AD, Mendelsohn J, Polikoff J, Sato GH. Biological effects in vitro of monoclonal antibodies to human epidermal growth factor receptors. *Mol Biol Med* 1983;1:511–529.
  39. Baron AT, Huntley BK, Lafky JM, Reiter JL, Liebenow J, McCormick DJ, Ziesmer SC, Roche PC, Mailhe NJ. Monoclonal antibodies specific for peptide epitopes of the epidermal growth factor receptor's extracellular domain. *Hybridoma* 1997;16:259–271.
  40. Elleman TC, Domagala T, McKern NM, Nerrie M, Lonnqvist B, Adams TE, Lewis J, Lovrecz GO, Hoyne PA, Richards KM, Howlett GJ, Rothacker J, Jorissen RN, Lou M, Garrett TP, Burgess AW, Nice EC, Ward CW. Identification of a determinant of epidermal growth factor receptor ligand-binding specificity using a truncated, high-affinity form of the ectodomain. *Biochemistry* 2001;40:8930–8939.
  41. King AC, Cuatrecasas P. Resolution of high and low affinity epidermal growth factor receptors. Inhibition of high affinity component by low temperature, cycloheximide, and phorbol esters. *J Biol Chem* 1982;257:3053–3060.
  42. Winkler ME, O'Connor L, Winget M, Fendly B. Epidermal growth factor and transforming growth factor alpha bind differently to the epidermal growth factor receptor. *Biochemistry* 1989;28:6373–6378.
  43. Soderquist AM, Carpenter G. Glycosylation of the epidermal growth factor receptor in A-431 cells. The contribution of carbohydrate to receptor function. *J Biol Chem* 1984;259:12586–12594.
  44. Kowalski JM, Parekh RN, Mao J, Wittrup KD. Protein folding stability can determine the efficiency of escape from endoplasmic reticulum quality control. *J Biol Chem* 1998;273:19453–19458.